Insect Biochemistry and Molecular Biology 147 (2022) 103798

Contents lists available at ScienceDirect

Insect Biochemistry and Molecular Biology

journal homepage: www.elsevier.com/locate/ibmb

Broad complex and wing development in cockroaches

Ana Fernandez-Nicolas [a,#], Alba Ventos-Alfonso [a,#], Orathai Kamsoi [a,1], Courtney Clark-Hachtel [b,2], Yoshinori Tomoyasu [b], Xavier Belles [a,*]

[a] Institute of Evolutionary Biology, CSIC-Universitat Pompeu Fabra, Barcelona, Spain
[b] Department of Biology, Miami University, 700E High St, Pearson Hall, Oxford, OH, 45056, USA

ARTICLE INFO

Keywords:
Broad complex
Wing-related genes
Initiation of wing development
Blattella
Nubbin

ABSTRACT

In hemimetabolan insects, the transcription factor Broad complex (Br–C) promotes wing growth and development during the nymphal period. We wondered whether Br–C could trigger the initiation of wing development, using the cockroach *Blattella germanica* as a model. We show that first instar nymphs have their unique identity of these three thoracic segments specified. During embryogenesis, the expression of *Br–C* and some wing-related genes show two matching waves. The first takes place before the formation of the germ band, which might be involved in the establishment of various developmental fields including a potential "wing field", and the second wave around organogenesis, possibly involved in the initiation of wing development. However, the expression of *Br–C* in early embryogenesis concentrates in the developing central nervous system, thus not co-localizing with the expression of the typical wing-related gene *vestigial*, which is expressed at the edge of the thoracic and abdominal segments. This suggests that Br–C is not specifically involved in the establishment of a potential "wing field" in early embryogenesis. Moreover, maternal RNAi for *Br–C* depletes the first wave of *Br–C* expression but does not affect the early expression of wing-related genes. As maternal *Br–C* RNAi did not deplete the second expression wave of *Br–C*, we could not evaluate if *Br–C* is involved in the initiation of wing development. Alternatively, using nymphal RNAi of *Br–C* and *Sex combs reduced* (*Scr*), we show that Br–C contributes to the formation of ectopic wing structures that develop in the prothorax when Scr is depleted. The gene most clearly influenced by *Br–C* RNAi is *nubbin* (*nub*), which, in nymphs is crucial for wing growth. Together, these results suggest that Br–C does not specifically contribute to the establishment of the "wing field", but it does seem important later, in the initiation of wing development, enhancing the expression of wing-related genes, especially *nub*. This supports the hypothesis previously proposed by the authors, whereby Br–C might have facilitated the evolution of holometaboly. However, there is no doubt that other factors have also contributed to this evolution.

1. Introduction

In insects, postembryonic development, and eventually the type of metamorphosis, is determined in the embryo. Considering metamorphosing insects, hemimetabolan species undergo a mode of development in which the embryo hatch into a first instar nymph that resembles a miniature adult. Then, the transformation into the adult stage essentially requires the development of mature wings and functional genitalia. In contrast, the embryogenesis of holometabolan species gives rise to a first instar larva that differs from the adult. This developmental mode requires a bridging stage between the larva and the adult, which is accomplished by the pupa (Belles, 2020). Therefore, if we want to study the mechanisms that determine the type of metamorphosis, we must look for them primarily in the embryo.

From an evolutionary point of view, two main theories have been proposed to explain the transition from hemimetaboly to holometaboly. One is the pronymph theory, which is rooted in the ideas of desembryonization proposed by Berlese (1913). Truman and Riddiford (1999) contend that holometabolan embryos "arrest" development at the so called pronymph stage and resume it during pupal development. Accordingly, the hemimetabolan pronymph would be homologous to all the holometabolan larval instars, while all hemimetabolan nymphal

* Corresponding author.
E-mail address: xavier.belles@ibe.upf-csic.es (X. Belles).
[1] Present address: Department of Biology, Faculty of Science and Technology, Chiang Mai Rajabhat University, Chiang Mai, Thailand.
[2] Present address: Department of Biology, University of North Carolina at Chapel Hill, Chapel Hill, NC, USA.
[#] These authors contribute equally to this work.

https://doi.org/10.1016/j.ibmb.2022.103798
Received 24 January 2022; Received in revised form 26 May 2022; Accepted 27 May 2022
Available online 1 June 2022

instars would be homologous to the pupa (Truman, 2019; Truman and Riddiford, 1999, 2019). The alternative is the theory of direct homology between stages, which is rooted in the ideas of Hinton (1963). This theory essentially posits that during holometabolan embryogenesis, the ancestral nymphal developmental program does not "arrest" but continues with the specifically adapted larval program. In this frame, the nymphal instars would be homologous to the larval instars, and the last larval instar homologous to the pupa (Belles, 2020; Huang et al., 2013; Jindra, 2019; Sehnal et al., 1996).

An important aspect of the evolution towards holometaboly is the suppression of wing development in juveniles, and the differentiation of them in the pupa. In this sense, and in the context of the theory of direct homology between stages, mechanisms facilitating the transition to holometaboly that involves the transcription factor Broad complex (Br–C) have been postulated. The *BR-C* gene encodes a BTB/POZ family of C2H2 zinc-finger transcription factors (DiBello et al., 1991). *Br–C* was discovered in *Drosophila melanogaster*, where it expresses four different transcripts that produce four protein isoforms (designated Z1 to Z4) which are believed to confer target specificity (DiBello et al., 1991). Mutation experiments revealed that *Br–C* is essential for proper ecdysone-regulated gene expression as larvae enter pupation (Kiss et al., 1988; von Kalm et al., 1994). In hemimetabolan nymphs, juvenile hormone (JH) promotes *Br–C* expression, which in turn promotes wing growth and development (Erezyilmaz et al., 2006; Huang et al., 2013; Konopová and Jindra, 2008). Conversely, JH represses *Br–C* expression in holometabolan larvae, so that Br–C begins to be significantly produced when JH production decreases in the prepupal stage, thus triggering the formation of the pupa, including the wings (Karim et al., 1993; Konopová and Jindra, 2008; Parthasarathy et al., 2008; Zhou et al., 1998). Br–C has been invoked by the proponents of the pronymph theory to explain the mechanisms that operated in the embryo that triggered the transition from nymphs to larvae (Erezyilmaz et al., 2006, 2009). According to this theory, the earlier appearance of JH in the holometabolan ancestors would have suppressed the onset of *Br–C* expression during embryonic development. Then, the absence of Br–C at the pronymphal molt "would freeze the proportions of the pronymph, resulting in a larva with more embryonic proportions" (Erezyilmaz et al., 2009). The essential idea is that Br–C might determine the formation of the nymph, just as it determines the formation of the pupa (Truman, 2019; Truman and Riddiford, 2019). In relation to Br–C, another mechanism that has been proposed to explain, at least in part, the origin of holometaboly would be a switch of the action of JH on *Br–C* expression, from stimulatory to repressor (Huang et al., 2013). This would determine that wing patterning and maturation would take place in the late larval period, as happens in many holometabolans.

A pertinent question that emerges from the reasoning of Huang et al. (2013) is whether Br–C determines the initiation of wing development and growth in the embryo, or if its action is restricted to the post-embryonic stages. It is in this context that we have explored here whether Br–C could directly induce the initiation of wing development, using a hemimetabolan model, the cockroach *Blattella germanica*, and the methodological approach of maternal and nymphal RNAi. Also, we have monitored the expression of a series of genes that, although they are pleiotropic, have key functions in wing development. The studied wing-related genes are as follows: *apterous-a* (*ap-a*), *nubbin* (*nub*), *scalloped* (*sd*), *Ultrabithorax* (*Ubx*), *vestigial* (*vg*) and *wingless* (*wg*). Of these, the one that has given the clearest results regarding the action of Br–C is *nub*.

Nub is a POU domain protein that has been mainly studied in *D. melanogaster*, where it plays an essential role in patterning and proximal-distal growth of the wing disc during late larval development (Cifuentes and Garcia-Bellido, 1997; Neumann and Cohen, 1998; Ng et al., 1995). Additionally, a diversity of roles of Nub have been reported in this fly, including the regulation of central nervous system (CNS) development, neuronal precursor cell division, specification of neuroblast temporal identity, cell fate lineage, and regulation of immune and tissue homeostasis (Tang and Engström, 2019). In relation with wing development, mutations in the *nub* gene in *D. melanogaster* result in adult phenotypes with a severe wing size reduction and pattern alterations, like transformations of distal elements into proximal ones (Cifuentes and Garcia-Bellido, 1997; Ng et al., 1995). Nub has been also studied in the paraneopteran and hemimetabolan species *Oncopeltus fasciatus*, where RNAi depletion triggered a reduction in the fore- and hindwing size, and a change in forewing shape (Medved et al., 2015).

2. Materials and methods

2.1. Insects and dissections

B. germanica specimens used in the experiments were from a colony reared in the dark at 30 ± 1 °C and 60–70% r.h. For RNA extractions, we used entire egg cases or oothecae (to establish the expression patterns along embryogenesis), or one of the three thoracic segments, the prothorax (T1), mesothorax (T2) or metathorax (T3) (in nymphs, using a pool of 10 segments per measurement). The respective entire segments T1, T2 or T3, were dissected, removing the haemocoel content, and subjected to extraction for quantitative real time PCR (qRT-PCR) measurements. For the *in situ* hybridization studies, we used individual embryos dissected out from 3-, 4- and 5-day-old oothecae. In the maternal RNAi experiments, freshly emerged females were maintained with males during the first gonadotrophic cycle; mating was confirmed at the end of experiments by assessing the occurrence of spermatozoids in the spermathecae. For dissections and tissue sampling, specimens were anesthetized with carbon dioxide.

2.2. Embryo staging

Expression studies were done throughout embryogenesis, from "Non fertilized eggs" (NFE) and embryo day 0 (ED0), to ED16. For staging, the morphological criteria of Tanaka (1976) and the molecular criteria of Ylla et al. (2018) have been used. As criteria, we also used juvenile hormone (JH) titers, based on data from Maestro et al. (2010) and titers of ecdysteroids (20E), according to data from Maestro et al. (2005).

2.3. RNA extraction and reverse transcription to cDNA

RNA extractions were carried out with RNeasy plant minikit (QIAGEN, Hilden, Germany) in the case of young oothecae (from 0- to 4-day-old), and HigherPurity™ tissue total RNA purification kit (Canvax Biotech, Cordoba, Spain), for older oothecae (from 6- to 16-day-old), and nymphs. The RNA extract of an entire ootheca (or a total of 400 ng of RNA in the case of nymphs) was treated with DNase (Promega, Madison, WI, USA) and reverse transcribed with Superscript II reverse transcriptase (Invitrogen, Carlsbad, CA, USA) and random hexamers (Promega). RNA quantity and quality were estimated by spectrophotometric absorption at 260 nm using a Nanodrop Spectrophotometer ND-1000® (452 NanoDrop Technologies, Wilmington, DE, USA).

2.4. Quantitative real-time PCR

Measurements with qRT-PCR were carried out in triplicate using an iQ5 Real-Time PCR Detection System (Bio-Rad Laboratories, Madrid, Spain), and SYBR®Green Supermix (iTaq™ Universal Supermix; Applied Biosystems, Madrid, Spain). In all measurement series, a control without a template was included. The primers used to measure the transcripts studied are indicated in Supplementary Table S1. The efficiency of the primers was validated by establishing a standard curve through four serial dilutions. mRNA levels were estimated relative to BgActin-5c expression, using the Bio-Rad iQ5 Standard Edition Optical System Software (version 2.0). Results are given as copies of mRNA per 1000 copies of BgActin-5c mRNA.

2.5. In situ hybridization

The procedure was originally reported by Clark-Hachtel et al. (2021) and is described in detail in Supplementary Table S2. Briefly, for embryo fixation, oothecae were removed from the female and placed in PBT in a microcentrifuge tube. They were then boiled at 100 °C for 10 min and dissected in 8% Formaldehyde/PBT with 1% EGTA to isolate embryos. Embryos were then fixed in this solution for 1 h at room temperature, washed with 100% methanol, and stored at −20 °C, at least overnight, before staining. The *Br–C*, *vg* and *dll* riboprobe templates were prepared from the respective cDNA fragment (Supplementary Table S1), and cloned into pCR4-TOPO via restriction digestion (NotI). In the case of *Br–C*, the riboprobe was designed within the core region, thus it would reveal all *Br–C* isoforms. The antisense riboprobes were synthesized with T3 polymerase and purified via ethanol precipitation. Before rehydration, embryos were treated with 1:1 (v/v) xylene:ethanol. After rehydration embryos were permeabilized with 80% acetone at −20 °C for 10 min and then post-fixed in 8% formaldehyde/PBS for 20 min at room temperature. The remaining steps are detailed in previously published protocol (Shippy et al., 2009; Tomoyasu et al., 2009), with the exception of the use of a ratio of 3:2000 riboprobe:hybridization buffer for hybridization and longer washes immediately following hybridization (two 3-h washes). Embryos were stained using Fast Red (Sigma F4648) for fluorescent imaging.

2.6. RNA interference

Procedures for dsRNA preparation were as described previously (Ciudad et al., 2006). A dsRNA from *Autographa californica* nucleopoydrovirus was used for control treatments (dsMock). The primers used to prepare the dsRNAs are detailed in Supplementary Table S3. Maternal RNAi treatments to target *Br–C* were carried out essentially as previously reported (Fernandez-Nicolas and Belles, 2017; Ventos-Alfonso et al., 2019). A volume of 1 μL of dsRNA solution (3 μg/μL), either of *Br–C* (dsBrC) or of control (dsMock) was injected into the abdomen of 5-day-old adult females. Then the effects of the treatment were examined at chosen days in the first ootheca, or in the first nymphal instar. Nymphal RNAi treatments were as previously described (Elias-Neto and Belles, 2016). In the single interference targeting *nub*, a volume of 1 μL of dsRNA solution (3 μg/μL) either of *nub* (dsnub) or of control (dsMock), was injected into the abdomen of nymphs. Three successive treatments were made, in the fourth, fifth and sixth (last) nymphal instar, freshly emerged in all cases. In the case of double interference targeting *Scr* and *Br–C*, the treatments were: a mixture of 0.5 μL of dsScr solution (6 μg/μL) plus 0.5 μL of dsBrC solution (6 μg/μL); a mixture of 0.5 μL of dsScr solution (6 μg/μL) plus 0.5 μL of dsMock solution (6 μg/μL); a mixture of 0.5 μL of dsBrC solution (6 μg/μL) plus 0.5 μL of dsMock solution (6 μg/μL); 1 μL of dsMock solution (6 μg/μL).

3. Results

3.1. Molecular differences in the thoracic segments of the first instar nymph

Firstly, we were interested in assessing whether the first instar nymphs already had determined the specific identity of the prothorax (T1), mesothorax (T2) and metathorax (T3). Our previous studies (Elias-Neto and Belles, 2016) had shown that in the sixth nymphal instar, previous to metamorphosis, the identity of each of the three thoracic segments is characterized by a combination of wing-related gene expression levels. Thus, at molecular level, T1 can be recognized by very high expression levels of *Sex combs reduced* (*Scr*), T3 by the very high expression levels of *Ubx*, while T2 is characterized with differential levels of expression of various genes with respect to T3, in particular by relatively high levels of *ap-a* expression. Moreover, the expression of other typical wing-related genes, like *nub*, *sd*, *vg* and *wg* is also characteristic of each segment. With these data in mind, we measured the expression of *ap-a*, *nub*, *Scr*, *sd*, *Ubx*, *vg* and *wg* in the respective thoracic segments T1, T2 and T3 of freshly emerged first instar nymphs. According to the expression of these genes, results confirm that the identity of the three segments is determined during embryogenesis, thus, they are molecularly differentiated in freshly emerged first instar nymphs. Therefore, T1 (no wings fate) is characterized by high expression of *Scr*, T2 (tegmina fate) by high expression of *apt-a* and *wg* with respect to T3, and T3 (membranous wings fate) by high expression of *Ubx* (Fig. 1A).

3.2. Broad complex and wing-related genes show two matching expression waves during embryogenesis

Then, we studied the expression of wing-related genes during embryo development. The expression pattern of *ap-a*, *nub*, *sd*, *Ubx* and *vg* show a wave in pre-blastoderm stage (ED1), and another one, more modest, around organogenesis (ED11-13). The expression of *wg* also shows a modest wave around ED11-13, but in early embryogenesis it acutely peaks on ED2 (Fig. 1B). The high levels of expression in early embryo led us to suspect that they could respond to an artifact derived from the low levels of actin-5C in early embryo stages (Piulachs et al., 2010). Therefore, we compared the qRT-PCR patterns of the wing-related genes with the transcriptomic profiles expressed in FPKM (Fragments Per Kilobase Million) reported by Ylla et al. (2018) for the same genes. The transcriptomic patterns (Fig. S1) show a reasonably good correspondence with those obtained by qRT-PCR (Fig. 1B), with relatively high values in early development (NFE, ED0 and ED1) and then decreasing in ED2 in almost all genes, or showing a peak in ED2 in the case of *wg*. A significant difference is in the *Ubx* pattern, which in ED6 and ED13 shows relatively higher transcriptomic values than qRT-PCRT values. However, the most significant discrepancy is the case of *ap*, with values that do not decrease beyond ED2. This is possibly due to the fact that *B. germanica*, as in other insects (Tomoyasu et al., 2009), has two *ap* genes, *ap-a* and *ap-b*, of which only *ap-a* is structurally characterized (GenBank: LT216431.1). Thus, the transcriptomic pattern (Fig. S1) shows a mixture of *ap-a* and *ap-b* expressions, while that of qRT-PCR (Fig. 1B) refers specifically to *ap-a*. Regarding *Br–C*, its expression pattern during embryogenesis shows a wave in pre-blastoderm stage (ED0), and another one, more modest, around organogenesis (ED13) (Figs. 1C and S2). The proportional distribution of the expression of the six isoforms of *Br–C* is similar in ED0 and ED6 (Fig. 1D).

3.3. Early Br–C expression localizes in the developing central nervous system of the embryo

Previous *in situ* hybridization studies in *B. germanica* embryos had shown that the first signs of *vg* expression can be observed in the brain on day 3 of development, while on day 4, *vg* expression becomes apparent at the edge of the dorsal terga throughout the thorax and abdomen (Clark-Hachtel et al., 2021). Thus, we chose day 4 embryos to compare the localization of expression of this typical wing-related gene with that of *Br–C* in early embryogenesis. To have another reference, we also determined the expression of *Distal-less* (*Dll*), a gene that typically promotes appendage development. As expected, *Dll* localizes in the distal end of the appendages, whereas *vg* mainly localizes at the edge of the three thoracic segments, as well as in the abdominal segments, as previously reported (Clark-Hachtel et al., 2021). In contrast, *Br–C* transcripts localize in the developing central nervous system, where the signal is especially clear in the cerebral ganglion, but also all along the ventral nerve cord (Fig. 2). The expression of *Br–C* in the cerebral ganglion is already visible at ED3 and persists at least until ED5 (Fig. S3). *In situ* hybridization studies in earlier embryo stages is limited by the huge amount of yolk proteins that hinder the hybridizations. On the other hand, on ED6 the second embryonic cuticle is formed (Piulachs et al.,

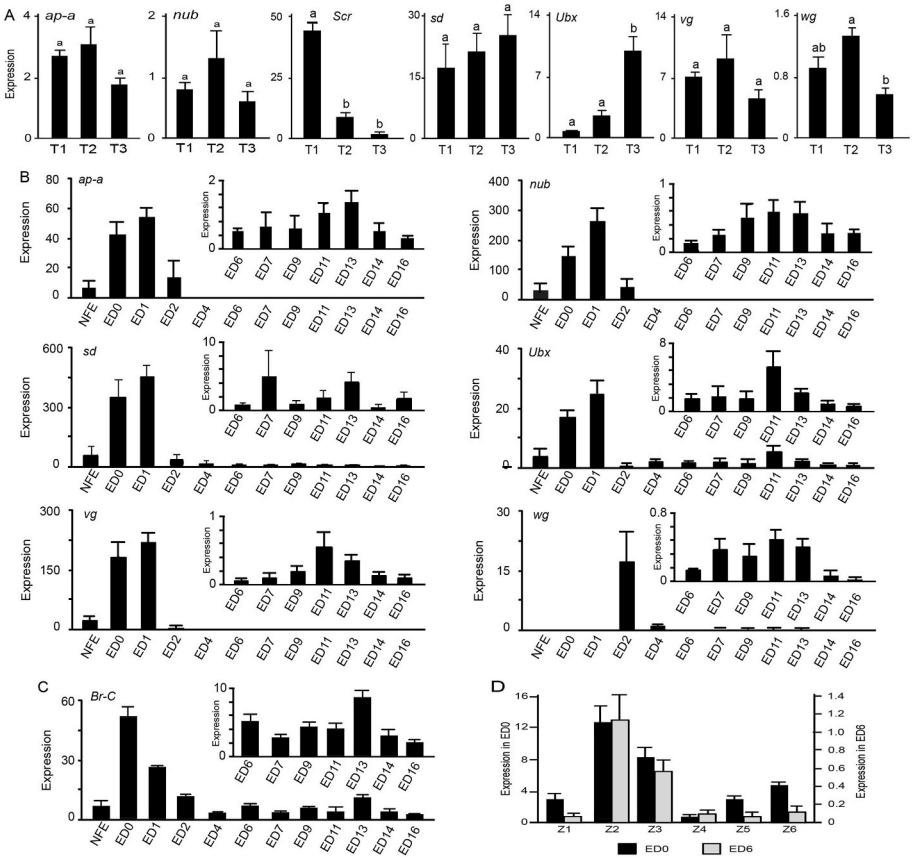

Fig. 1. Expression of *Broad complex* (*Br–C*) and the wing-related genes *apterous-a* (*ap-a*), *nubbin* (*nub*), *scalloped* (*sd*), *Sex combs reduced* (*Scr*), *Ultrabithorax* (*Ubx*), *vestigial* (*vg*) and *wingless* (*wg*) in *Blattella germanica*. (A) Expression of wing-related genes in the prothorax (T1), mesothorax (T2), and metathorax (T3) of the first nymphal instar (N1). (B) Expression of wing-related genes during embryogenesis; from non-fecunded eggs stage (NFE) to embryo day 16 (ED16). (C) Expression of *Br–C* during embryogenesis. (D) Expression of the *Br–C* isoforms Z1 to Z6 in ED0 and ED6. In C and B, the inset shows the expression from ED6 to ED16 in detail. Expression is represented as mRNA copies per 1000 copies of actin-5c (mean ± SEM, n = 3–4); in A, different letters indicate statistically significant differences ($p < 0.05$), according to ANOVA test, followed by DUNCAN's HSD post hoc test.

Fig. 2. Localization of selected transcripts by *in situ* hybridization (ISH) in embryos of *Blattella germanica*. ISH was carried out on 4-day-old embryos (ED4) for the transcripts of *vestigial* (*vg*) (dorso-lateral view), *Distal-less* (*Dll*) (ventral view) and *Broad complex* (*Br–C*) (ventral view). blue: DAPI staining; red: ISH labeling. The *Br–C* riboprobe was designed within the core region, thus it reveals all *Br–C* isoforms. Scale: 200 μm.

2010), which prevents the penetration of reagents for *in situ* hybridization. Therefore, we were also unable to obtain information about expression localization beyond ED6, in particular during the second wave of expression of Br–C and wing-related genes around ED13.

3.4. Maternal RNAi of Br–C depletes the first wave of Br–C expression in the embryo but does not significantly affect the early expression of wing-related genes

The effects of maternal RNAi of *Br–C* in *B. germanica* had been previously studied by Piulachs et al. (2010). Here we focused our attention on the duration of the RNAi effects in terms of quantitatively measured transcript decrease, and how this affects the expression of wing-related genes. Thus, 5-day-old adult females were injected with 3 μg of dsBrC (treated females), or with 3 μg of dsMock (control females) and kept with males until the formation of the first ootheca, which took place three days post-injection in both groups. Using different batches, oothecae were dissected when freshly formed (ED0), and on days 1, 2, 6 and 13 (ED1 to ED13). An additional stage was non-fertilized eggs (NFE), obtained from the female just before ovulation (Ylla et al., 2018). Then, we measured the levels of *Br–C* mRNA in these stages by qRT-PCR. We found that *Br–C* transcript levels were reduced in treated samples in ED0, ED1 and ED2 (Fig. 3A). We already knew that the action of maternal RNAi produced an efficient reduction of *Br–C* transcripts in ED4 (Piulachs et al., 2010). However, and according to the present experiments, maternal RNAi of *Br–C* is no longer efficient in the embryo from ED6 onwards (Fig. 3A). At the level of *Br–C* isoforms, when the expression is measured in ED0, the results show that it is reduced in all of them, while when it is measured in ED6, no statistically significant effects are observed in any of the isoforms (Fig. 3B). The phenotypes obtained in our experiments of maternal RNAi of *Br–C* were similar to those previously reported (Piulachs et al., 2010). Most of the malformed embryos interrupted development very early, around the formation of the germ band anlage (Supplementary Figs. S4 and S5). Supplementary Table S4 summarizes the experiments performed and the results obtained.

We then studied the effect of maternal RNAi of *Br–C* in the first expression wave of wing-related genes. Their mRNA levels were measured in ED1 in both control and treated embryos, except that of *wg*, which was measured in ED2 according to the expression patterns previously obtained (Fig. 1B). We confirmed that *Br–C* expression was effectively depleted, as expected, but no significant differences were observed between controls and treated regarding the expression of any of the wing-related genes (Fig. 3C). We also did not find significant differences between controls and treated in the expression of wing-related genes in freshly hatched first nymphal instar (Fig. 3D).

3.5. Br–C contributes to the development of ectopic wing structures in the prothorax after depleting Scr in nymphs

An alternative strategy to see if Br–C is needed to initiate wing development in *B. germanica* would be to induce ectopic development of wing structures in T1 through the RNAi of *Scr* (Clark-Hachtel et al., 2021; Elias-Neto and Belles, 2016). The idea was to see whether the additional RNAi of *Br–C* would impair this ectopic wing development. Accordingly, we treated nymphs with dsScr, or dsScr plus dsBrC in the fourth, fifth and sixth nymphal instars. We did the equivalent experiment treating with dsBrC alone, as a reference. Controls were treated in parallel with dsMock.

We measured the decrease of the respective transcripts in T1 on N6D6, since it is the stage in which the metamorphic peak of ecdysone occurs (Romaña et al., 1995), and the wing maturation in T2 and T3 is triggered (Huang et al., 2013). Results (Fig. 4A) showed that the different treatments depleted the targeted transcript(s). Intriguingly, Scr depletion reduced *Br–C* mRNA levels by 38%, suggesting that Scr directly or indirectly enhances *Br–C* expression. Regarding the effects on

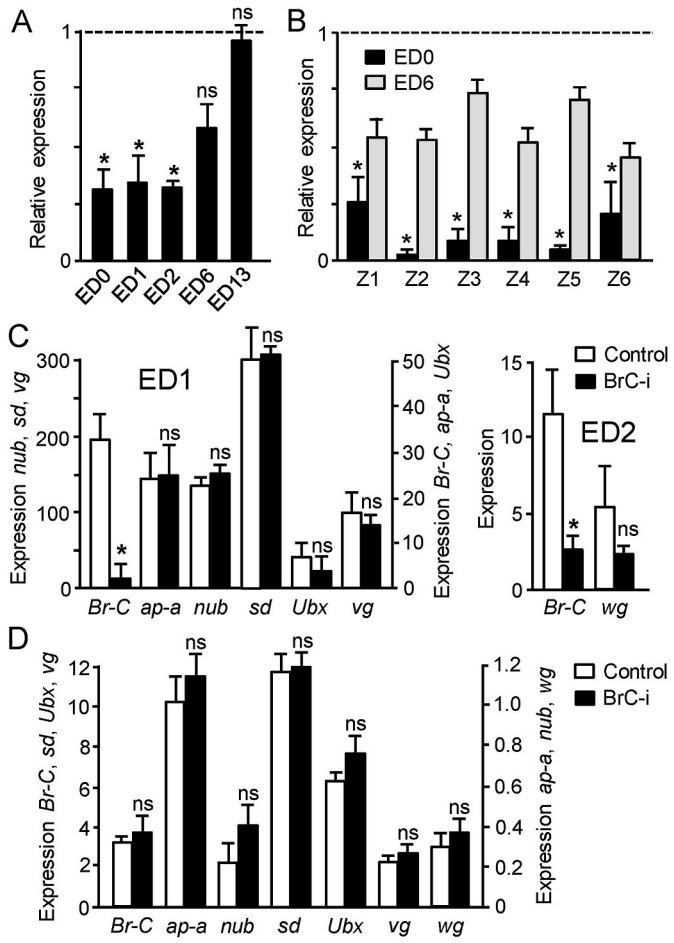

Fig. 3. Effects of maternal RNAi of *Broad complex* (*Br–C*) in *Blattella germanica* in terms of transcript decrease and wing-related genes expression. (A) *Br–C* transcript decrease after maternal RNAi in embryos of different ages, from day 0 (ED0) to day 13 (ED13). (B) Transcript decrease of the different isoforms of *Br–C* (Z1 to Z6) in ED0 and ED6. (C) Expression of *apterous-a* (*ap-a*), *nubbin* (*nub*), *scalloped* (*sd*), *Ultrabithorax* (*Ubx*), and *vestigial* (*vg*) in ED1, and *wingless* (*wg*) on ED2, from females treated with dsBrC (BrC-i) and with dsMock (Control); in both ages, the transcript decrease of *Br–C* is shown. (D) Expression of *apt-a*, *Br–C*, *nub*, *sd*, *Ubx*, *vg*, and *wg*, in freshly emerged first instar nymphs, from females treated with dsBrC and control females (dsMock-treated). Expression is represented as mRNA copies per 1000 copies of actin-5c (mean ± SEM, n = 3–4); in A and B, the mRNA levels are normalized with respect to respective control values (indicated as 1); the asterisk indicates statistically significant differences with respect to controls ($p < 0.05$), according to REST (Pfaffl et al., 2002); n.s. means not statistically significant.

wing-related genes, their expression generally increased in T1 after depleting *Scr*, as previously reported (Elias-Neto and Belles, 2016). The increase was statistically significant in *nub* and *vg*, while a tendency to increase was observed in the case of *ap-a*, *sd*, *Ubx* and, especially, *wg* (Fig. 4B). The simultaneous treatment with dsBrC impaired the upregulation of wing-related genes in dsScr-treated insects, especially *nub*, *vg* and *wg*, whose expression increased between 73 and 89% less than when treated only with dsScr. Of these three genes, *nub* showed statistically significant differences, possibly because its expression is the most dramatically stimulated in T1 when Scr is depleted (Elias-Neto and Belles, 2016). As expected, depletion of *Br*–C alone did not significantly affect the expression of wing-related genes in T1 (Fig. 4B).

Morphologically, the adults emerging from dsMock-treated nymphs had the pronotum slightly transverse, with rounded sides, with the maximum width below the middle, and showing the disc uniformly convex (Fig. 4C). In contrast, those emerging from dsScr-treated nymphs

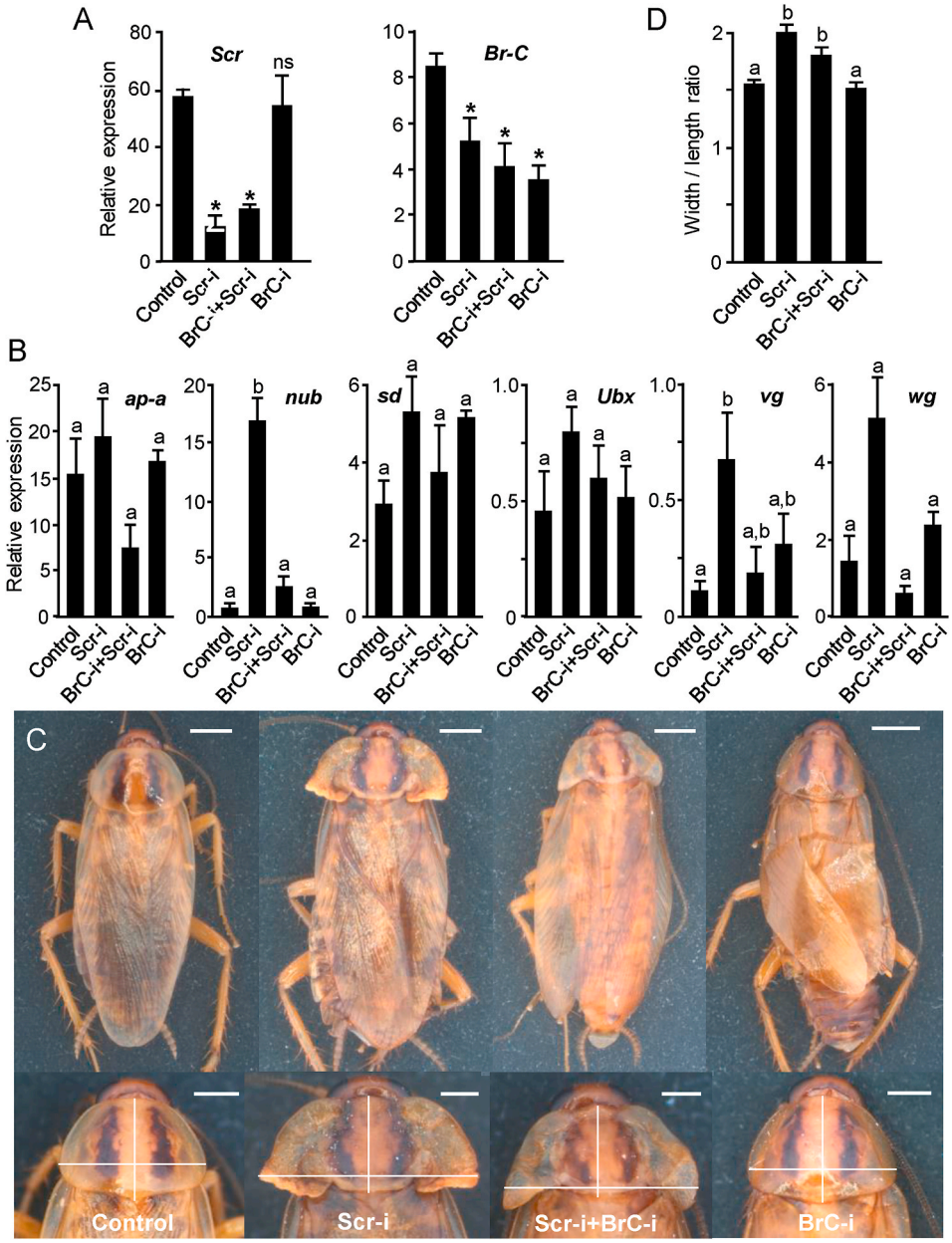

Fig. 4. Effects of the double RNAi of *Broad complex* (*Br–C*) and *Sex combs reduced* (*Scr*) in terms of wing-related gene expression and prothorax phenotype in *Blattella germanica*. (A) *Br–C* and *Scr* transcript decrease after nymphal RNAi; insects where treated with 6 μg of dsMock (Control), a mixture of 3 μg of dsScr plus 3 μg of dsMock (Scr-i), a mixture of 3 μg of dsScr plus 3 μg of dsBrC (Scr-i + BrC-i), or a mixture of 3 μg of dsBrC plus 3 μg of dsMock (BrC-i), in 1 μL of dsRNA solution in all cases. The respective treatment was made in fourth, fifth, and sixth freshly ecdysed nymphal instars, and transcript decrease was measured on 6-day-old sixth instar nymphs (N6D6). (B) Effects of the nymphal RNAi on the expression of *apterous-a* (*ap-a*), *nubbin* (*nub*), *scalloped* (*sd*), *Ultrabithorax* (*Ubx*), *vestigial* (*vg*), and *wingless* (*wg*) in the prothorax (T1), as measured on N6D6. (C) Phenotypes resulting from nymphal RNAi of *Br–C* and *Scr*; in the bottom images, which show the detail of the pronotum, we have indicated with white lines where the length and width measurements were made; scale: 1 mm (insect), or 2 mm (pronotum). (D) Effects of the nymphal RNAi of *Br–C* and *Scr* on the width/length ratio of the pronotum. In A and B, expression is represented as mRNA copies per 1000 copies of actin-5c, mean ± SEM, n = 3–4; in C, the pronotum width/length ratio is represented as mean ± SEM, n = 18–22; in A, the asterisk indicates statistically significant differences ($p < 0.05$) of each treatment with respect to controls (dsMock-treated) according to REST (Pfaffl et al., 2002), and n.s. means not statistically significant; in B and D, different letters indicate statistically significant differences ($p < 0.05$), according to ANOVA test, followed by DUNCAN's HSD post hoc test.

had a clearly transverse pronotum, with its maximum width practically at the base, and showing conspicuous latero-posterior expansions of the pronotal edge, such as those described by Elias-Neto and Belles (2016) and Clark-Hachtel et al. (2021). Although with some variability, the latero-posterior expansions were consistently large, and showed a wrinkled lobular basal structure. Moreover, the pronotum showed two longitudinal grooves separating the actual pronotal disc from the latero-posterior expansions, which ended at the base with respective notches (Fig. 4C). Interestingly, the latero-posterior expansions of the pronotum triggered by *Scr* depletion tended to be smaller in the insects in which *Br–C* was also depleted, although no qualitative differences were observed. The pronotum was less transverse, and the latero-posterior expansions were less pronounced, with a practically smooth basal lobular structure. In addition, the longitudinal grooves separating the disc from the latero-posterior expansions, and the respective basal notches, were less marked (Fig. 4C). As expected, the adults emerging from dsBrC- and dsScr + dsBrC-treated nymphs showed a reduction in T2 tegmina and T3 membranous wings, a feature typical of *Br–C* knockdowns (Huang et al., 2013) (Fig. 4C). Biometrically, although the differences between the relative width of the pronotum (width/length ratio) of *Scr*-depleted and *Scr* + *Br–C*-depleted insects were not statistically significant, the relative width of the pronotum in *Scr*-depleted adults increased by 31% on average compared to the controls, while it increased by 19% in *Scr* + *Br–C*-depleted (Fig. 4D). Supplementary Table S5 summarizes the experiments performed and the results obtained.

3.6. *Br–C and nubbin in wing development*

Of all the genes studied, *nub* stands out for dramatically increasing its expression in T1 after depleting *Scr* and for the robust contribution of *Br–C* to this increase. Thus, we decided to study the role of *nub* in wing development in *B. germanica*. In T1, *nub* is practically not expressed (Elias-Neto and Belles, 2016). In T2 and T3, its expression in the last nymphal instar (N6) shows a similar pattern: increasing until day 4 and then decreasing until practically vanishing on day 8 (Fig. 5A), that is just before molting to adult. Therefore, to study the contribution of *nub* to wing development, we did nymphal RNAi experiments by treating

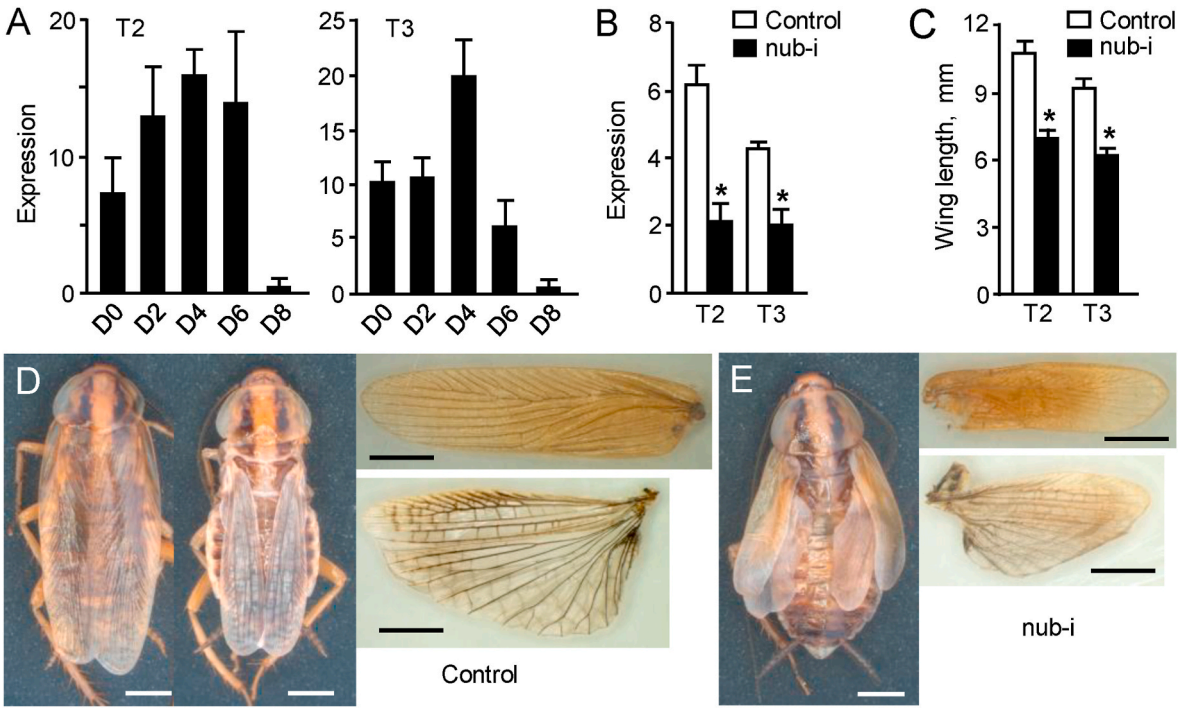

Fig. 5. Expression of *nubbin* (*nub*) in *Blattella germanica* and effects of nymphal RNAi. (A) Expression of *nub* in the mesothorax (T2) and metathorax (T3) from day 0 (D0) to day 8 (D8) of the last nymphal instar. (B) *nub* transcript decrease after nymphal RNAi in day 6 of the last nymphal instar as measured in T2 and T3; insects where treated with 3 μg of dsMock (Control), or 3 μg of dsnub (nub-i) in 1 μL of dsRNA solution in both cases. The respective treatment was made in fourth, fifth, and sixth freshly ecdysed nymphal instars, and transcript decrease was measured on 6-day-old sixth instar nymphs (N6D6). (C) Effects of the nymphal RNAi of *nub* on the length of the T2 and T3 wings. (D–E) Phenotype resulting from nymphal RNAi of *nub* (E) compared with controls (D); in controls the dorsal view of the insect is shown with the tegmina in place (left) and with the tegmina removed (right), to uncover the membranous wing in place; in controls and treated, the isolated tegmina, and the isolated membranous wing is also shown. In A and B, expression is represented as mRNA copies per 1000 copies of actin-5c (mean ± SEM, n = 3–4); in C, wing length is represented as mean ± SEM, n = 8–18; in A, B and C the asterisk indicates statistically significant differences with respect to controls ($p < 0.05$), according to REST (Pfaffl et al., 2002) (A, B) or student's *t*-test (C). In D and E, scale: 2 mm.

freshly ecdysed fourth, fifth, and sixth nymphal instars with dsnub. Expression measurements on N6D6 showed that *nub* transcript levels had been significantly lowered by the dsnub treatment (Fig. 5B). At a phenotypic level, the resulting adults showed a reduction in the tegmina and membranous wings (Fig. 5C). In dsMock-treated controls, both the tegmina and the membranous wings clearly exceed the apical part of the abdomen (Fig. 5D), whereas in dsnub-treated insects both pairs of wings are shorter than the abdomen (Fig. 5E). Otherwise, both the tegmina and the membranous wings show a vein pattern essentially the same as the controls. Supplementary Table S5 summarizes the experiments performed and the results obtained. The wings of nub-depleted adults (Fig. 5E) are similar in size and general shape to those observed in Br–C-depleted adults (Fig. 4C). However, those of the latter have severe defects in the venation pattern and show a shorter CuP vein and an associated notch at the wing edge, as described in detail by Huang et al. (2013), which are not present in dsnub-treated insects.

4. Discussion

4.1. Wing identity fate in different thoracic segments is specified during embryogenesis

The freshly emerged first instar nymphs appear to have T1, T2 and T3 differentiated, according to the combination of the expression levels of wing-related genes in these segments. Thus, the identity of T1 (no wings fate; high *Scr* expression), T2 (tegmina fate; high expression of *wg* and *ap-a* in relation to T3), and T3 (membranous wings fate; high *Ubx* expression) is specified during embryogenesis. In the embryo, we have seen that there are two waves of wing-related gene expression. The first occurs in early embryogenesis on days 0 and 1 at 0–6% development, thus in Tanaka stage 1, before the formation of the germ band (Tanaka, 1976). The second expression wave, which is more modest, occurs in the last third of embryogenesis around day 13 (72% development), thus in Tanaka stage 15, before organogenesis. Intriguingly, these two waves coincide with respective waves of *Br–C* expression, and the second one with the last and most intense embryonic peak of ecdysteroid levels, as measured by Maestro et al. (2005).

The question is whether the first or second wave of expression of these wing-related genes is related to the initiation of wing development. In this context, we must bear in mind that what we call "wing-related genes" are highly pleiotropic, so that these genes also have functions other than promoting wing development; for example, all of them are also related to some aspect of neural development (Berndt et al., 2015; Corty et al., 2016; Gabilondo et al., 2018; Kawamura et al., 2021; Tidswell et al., 2021). Regarding *nub*, it has been described that, in the milkweed bug *O. fasciatus*, this gene contributes to antenna morphogenesis, labial patterning, the length of the femoral segment in legs, and the formation of a limbless abdomen (Hrycaj et al., 2008). In contrast, in the house cricket *Acheta domestica*, and the American cockroach *Periplaneta americana*, *nub* plays an important role in antennae and leg patterning but does not seem to participate in the morphogenesis of the mouthparts and the abdomen (Turchyn et al., 2011). In addition, a close examination of *nub* functions in *D. melanogaster* has revealed that, apart from its classical functions in wing development, it also contributes to leg patterning (Turchyn et al., 2011). Therefore, the expression patterns alone cannot inform whether the first and/or the second expression wave of wing-related genes promotes the initiation of wing development. What we do know is that tergal expression of *vg* starts in ED4 of *B. germanica* embryogenesis (Clark-Hachtel et al., 2021), which suggests that the "wing field" begins

to be determined around this time. However, we presume that more genetic inputs are needed to induce the initiation of wing development in T2 and T3. These additional genetic inputs could occur around ED13, coinciding with the last and major pulse of ecdysteroid production and *Br–C* expression, and the second wave of expression of wing-related genes.

4.2. Maternal RNAi does not reveal whether Br–C is required for the initiation of wing development in the embryo

Our results have shown that maternal RNAi reduces the *Br–C* transcripts of the first expression wave, but not the second, as transcript decrease effects do not persist beyond ED6 (33% development). However, depletion of early Br–C mRNA levels generally did not affect the first expression wave of wing-related genes. Intriguingly, our *in situ* hybridization studies show that *vg* expression in ED4 localizes at the edge of the dorsal terga of the thoracic and abdominal segments, whereas that of *Br–C* appears to be restricted to the developing CNS in the same stage. This disparate location suggests that, if a "wing field" is established in early embryogenesis, Br–C does not appear to specifically contribute to this process. Regarding the second wave of wing-related gene expression around ED13, our results showed that the transcript decrease effects of maternal RNAi vanish from ED6. Thus, this RNAi approach does not reveal if Br–C is required for the initiation of wing development in the embryo. What is clear, however, is that early *Br–C* transcripts are important for the formation of the germ band, as already demonstrated by Piulachs et al. (2010) and corroborated again here. The inability to form the germ band in *Br–C* depleted early embryos is reminiscent of the phenotypes obtained by impairing JH signaling in the embryo (Fernandez-Nicolas and Belles, 2017), which is not surprising as such depletion led to reduced *Br–C* expression.

4.3. Br–C contributes to the formation of ectopic wing structures in T1

In *B. germanica*, RNAi of *Scr* in nymphs, increases the expression of wing-related genes in T1, most notably that of *nub*, and wing-like structures are formed in this segment (Clark-Hachtel et al., 2021; Elias-Neto and Belles, 2016). Here we have shown that the additional depletion of *Br–C* impairs the increased expression of wing-related genes in T1, in a statistically significant way in the case of *nub*. At a phenotypic level, no detailed patterning (like venation) is discernible in the ectopic T1 wing structures, but at least in terms of size, they are smaller in insects where both *Scr* and *Br–C* have been depleted, than in those where only *Scr* was depleted. Interestingly, this is similar to some observations in *O. fasciatus*, in which the double depletion of *Scr* and *nub* produced much less development of ectopic wing structures in T1 than was obtained by only depleting *Scr* (Medved et al., 2015). It should be noted that the size of the ectopic wing structures in the insects treated with dsScr plus dsBrC is not much smaller (a 12% difference) than that of those treated with dsScr alone. However, it must be remembered that treatment with only dsScr, apart from effectively reducing the expression of Scr (79%), also reduces that of Br–C (38%). This result helps to interpret why the size of the ectopic wing structures in insects treated with dsScr plus dsBrC is not much smaller than that of those treated with dsScr alone.

Again in terms of size, the RNAi experiments in nymphs of *B. germanica* reported herein revealed that *nub* promotes the global growth of tegmina and membranous wings, results that are reminiscent to those obtained in *D. melanogaster* (Cifuentes and Garcia-Bellido, 1997; Ng et al., 1995) and *O. fasciatus* (Medved et al., 2015). The data suggests that *nub* is strongly involved in the growth of ectopic wing structures in T1, and in the current wing growth in T2 and T3 in hemimetabolan species.

It is worth noting that reduced adult wing size was the only defect observed in *B. germanica* after depleting *nub* in nymphs. This differs from the phenotype observed when depleting *Br–C* under similar conditions, which is more complex. In the *Br–C* depleted insects, the wings, especially those of T3, are smaller, have a shorter CuP vein (leaving a notch in the wing edge at the CuP end), and show disorganized vein/inter-vein patterning in the anterior part, and broken A-veins, especially in the posterior part (Huang et al., 2013). The role of Br–C in vein/intervein patterning appears to be mediated by the miRNAs let-7 and miR-100 (Rubio and Belles, 2013), whereas the mechanism that determines the correct formation of the CuP is unknown, although we can suppose that the action of Br–C would also be indirect, perhaps mediated by wing and vein patterning genes. Thus, in addition to promoting *nub* expression and general growth, Br–C plays other roles related to wing differentiation and patterning.

4.4. Br–C, wing development, and the evolution of metamorphosis

As stated in the introduction, we had proposed that Br–C may have been instrumental in the evolution of holometabolan metamorphosis (Belles, 2020; Huang et al., 2013). Thus, an important event in the transition from hemimetaboly to holometaboly could have been a switch in the action of JH on *Br–C* expression from stimulatory (hemimetabolans) to inhibitory (holometabolans). This would determine that the onset of wing patterning and maturation would take place in the late larval period and pupal stage, when JH production vanishes and *Br–C* expression is significantly upregulated (Belles, 2020; Huang et al., 2013). Taken together, the evidence suggests that in the hemimetabolan *B. germanica*, Br–C is important in the initiation of wing development, in their growth, and patterning through the promotion of wing-related gene expression. This affords additional support to the above hypothesis, although we also believe that other factors must also have contributed to the evolution of holometaboly. For example, when comparing the ontogenetic series of transcriptomes of *B. germanica* and *D. melanogaster* (Ylla et al., 2018), it can be observed that there are more than 90 genes with morphogenesis-related functions that are expressed differently during embryo development in both species. Thus, in early embryogenesis, a number of them are highly expressed in *B. germanica* and little or not at all in *D. melanogaster*, and vice versa, while the same happens to other genes in mid-late embryogenesis (Ylla et al., 2018). Further functional studies of genes differentially expressed in the embryo of hemimetabolan and holometabolan species will provide valuable information on the factors that contributed to determine the evolutionary transition between these two types of metamorphosis, which involved the emergence of the larval stage.

Data availability

Data will be made available on request.

Acknowledgements

The work of Xavier Belles was supported by the Spanish Agencia Estatal de Investigación (grant number PID2019-104483 GB-I00/AEI/10.13039/501100011033; CGL2015-64727-P; and CGL2012-36251), including support for the visit of Ana Fernandez-Nicolas to the Tomoyasu lab), the Catalan Government (2017 SGR 1030), and European Fund for Economic and Regional Development (FEDER funds). The work of Yoshinori Tomoyasu was supported by the Miami University Faculty Research Grants Program (CFR), the National Science Foundation (NSF; IOS1557936), and an NSF Graduate Research Fellowship to Courtney Clark-Hachtel. The authors thank the Center for Advanced Microscopy and Imaging (CAMI) at Miami University for technical support. Thanks are also due to the three anonymous reviewers for the effort they have dedicated to our manuscript, which has contributed significantly to its improvement.

Appendix A. Supplementary data

Supplementary data to this article can be found online at https://doi.org/10.1016/j.ibmb.2022.103798.

References

Belles, X., 2020. Insect Metamorphosis. From Natural History to Regulation of Development and Evolution. Academic Press, London.

Berlese, A., 1913. Intorno alle metamorfosi degli insetti. Redia 9, 121–136.

Berndt, A.J., Tang, J.C., Ridyard, M.S., Lian, T., Keatings, K., Allan, D.W., 2015. Gene regulatory mechanisms underlying the spatial and temporal regulation of target-dependent gene expression in *Drosophila* neurons. PLoS Genet 11, e1005754.

Cifuentes, F.J., Garcia-Bellido, A., 1997. Proximo-distal specification in the wing disc of *Drosophila* by the *nubbin* gene. Proc. Natl. Acad. Sci. U S A 94, 11405–11410.

Ciudad, L., Piulachs, M.-D., Belles, X., 2006. Systemic RNAi of the cockroach vitellogenin receptor results in a phenotype similar to that of the *Drosophila* yolkless mutant. FEBS J 273, 325–335. https://doi.org/10.1111/j.1742-4658.2005.05066.x.

Clark-Hachtel, C., Fernandez-Nicolas, A., Belles, X., Tomoyasu, Y., 2021. Tergal and pleural wing-related tissues in the German cockroach and their implication to the evolutionary origin of insect wings. Evol. Dev. 23, 100–116.

Corty, M.M., Tam, J., Grueber, W.B., 2016. Dendritic diversification through transcription factor-mediated suppression of alternative morphologies. Development 148, 1351–1362.

DiBello, P.R., Withers, D.A., Bayer, C.A., Fristrom, J.W., Guild, G.M., 1991. The *Drosophila* broad-complex encodes a family of related proteins containing zinc fingers. Genetics 129, 385–397.

Elias-Neto, M., Belles, X., 2016. Tergal and pleural structures contribute to the formation of ectopic prothoracic wings in cockroaches. R. Soc. Open Sci. 3, 160347. https://doi.org/10.1098/rsos.160347.

Erezyilmaz, D.F., Riddiford, L.M., Truman, J.W., 2006. The pupal specifier broad directs progressive morphogenesis in a direct-developing insect. Proc. Natl. Acad. Sci. U. S. A. 103, 6925–6930.

Erezyilmaz, D.F., Rynerson, M.R., Truman, J.W., Riddiford, L.M., 2009. The role of the pupal determinant broad during embryonic development of a direct-developing insect. Dev. Genes Evol. 219, 535–544. https://doi.org/10.1007/s00427-009-0315-7.

Fernandez-Nicolas, A., Belles, X., 2017. Juvenile hormone signaling in short germ-band hemimetabolan embryos. Development 144, 4637–4644. https://doi.org/10.1242/dev.152827.

Gabilondo, H., Rubio-Ferrera, I., Losada-Pérez, M., Del Saz, D., León, Y., Molina, I., Torroja, L., W, D., J, A., S, B., 2018. Segmentally homologous neurons acquire two different terminal neuropeptidergic fates in the *Drosophila* nervous system. PLoS One 13, e0194281.

Hinton, H.E., 1963. The origin and function of the pupal stage. Proc. R. Entomol. Soc. London 38, 77–85.

Hrycaj, S., Mihajlovic, M., Mahfooz, N., Couso, J.P., Popadić, A., 2008. RNAi analysis of nubbin embryonic functions in a hemimetabolous insect, *Oncopeltus fasciatus*. Evol. Dev. 10, 705–716. https://doi.org/10.1111/j.1525-142X.2008.00284.x.

Huang, J.-H., Lozano, J., Belles, X., 2013. Broad-complex functions in postembryonic development of the cockroach *Blattella germanica* shed new light on the evolution of insect metamorphosis. Biochim. Biophys. Acta - Gen. Subj. 1830, 2178–2187. https://doi.org/10.1016/j.bbagen.2012.09.025.

Jindra, M., 2019. Where did the pupa come from? The timing of juvenile hormone signalling supports homology between stages of hemimetabolous and holometabolous insects. Philos. Trans. R. Soc. B 374, 20190064.

Karim, F.D., Guild, G.M., Thummel, C.S., 1993. The *Drosophila* Broad-Complex plays a key role in controlling ecdysone-regulated gene expression at the onset of metamorphosis. Development 118, 977–988.

Kawamura, H., Hakeda-Suzuki, S., Suzuki, T., 2021. Activity-dependent endocytosis of Wingless regulates synaptic plasticity in the *Drosophila* visual system. Genes Genet. Syst. 95, 235–247.

Kiss, I., Beaton, A.H., Tardiff, J., Fristrom, D., Fristrom, J.W., 1988. Interactions and developmental effects of mutations in the Broad-Complex of *Drosophila melanogaster*. Genetics 118, 247–259.

Konopová, B., Jindra, M., 2008. Broad-Complex acts downstream of Met in juvenile hormone signaling to coordinate primitive holometabolan metamorphosis. Development 135, 559–568. https://doi.org/10.1242/dev.016097.

Maestro, J.L., Pascual, N., Treiblmayr, K., Lozano, J., Belles, X., 2010. Juvenile hormone and allatostatins in the German cockroach embryo. Insect Biochem. Mol. Biol. 40, 660–665. https://doi.org/10.1016/j.ibmb.2010.06.006.

Maestro, O., Cruz, J., Pascual, N., Martín, D., Belles, X., 2005. Differential expression of two RXR/ultraspiracle isoforms during the life cycle of the hemimetabolous insect *Blattella germanica* (Dictyoptera, Blattellidae). Mol. Cell. Endocrinol. 238, 27–37. https://doi.org/10.1016/j.mce.2005.04.004.

Medved, V., Marden, J.H., Fescemyer, H.W., Der, J.P., Liu, J., Mahfooz, J., Popadić, A., 2015. Origin and diversification of wings: insights from a neopteran insect. Proc. Natl. Acad. Sci. U S A 112, 15946–15951.

Neumann, C.J., Cohen, S.M., 1998. Boundary formation in *Drosophila* wing: notch activity attenuated by the POU protein Nubbin. Science 281, 409–413.

Ng, M., Diaz-Benjumea, F.J., Cohen, S.M., 1995. *Nubbin* encodes a pou-domain protein required for proximal-distal patterning in the Drosophila wing. Development 121, 589–599.

Parthasarathy, R., Tan, A., Bai, H., Palli, S.R., 2008. Transcription factor broad suppresses precocious development of adult structures during larval-pupal metamorphosis in the red flour beetle. *Tribolium castaneum*. Mech. Dev. 125, 299–313.

Pfaffl, M.W., Horgan, G.W., Dempfle, L., 2002. Relative expression software tool (REST) for group-wise comparison and statistical analysis of relative expression results in real-time PCR. Nucleic Acids Res 30, e36.

Piulachs, M.-D., Pagone, V., Belles, X., 2010. Key roles of the *Broad-Complex* gene in insect embryogenesis. Insect Biochem. Mol. Biol. 40, 468–475. https://doi.org/10.1016/j.ibmb.2010.04.006.

Romaña, I., Pascual, N., Belles, X., 1995. The ovary is a source of circulating ecdysteroids in *Blattella germanica*. Eur. J. Entomol. 93, 93–103.

Rubio, M., Belles, X., 2013. Subtle roles of microRNAs let-7, miR-100 and miR-125 on wing morphogenesis in hemimetabolan metamorphosis. J. Insect Physiol. 59, 1089–1094. https://doi.org/10.1016/j.jinsphys.2013.09.003.

Sehnal, F., Švácha, P., Zrzavý, J., 1996. Evolution of insect metamorphosis. In: Gilbert, L. I., Tata, J.R., Atkinson, B.G. (Eds.), Metamorphosis. Postembryonic Reprogramming of Gene Expression in Amphibian and Insect Cells. Academic Press, San Diego, pp. 3–58.

Shippy, T.D., Coleman, C.M., Tomoyasu, Y., Brown, S.J., 2009. Concurrent in situ hybridization and antibody staining in red flour beetle (*Tribolium*) embryos. Cold Spring Harb. Protoc. 2009, pdb.prot5257 https://doi.org/10.1101/Pdb.Prot5257.

Tanaka, A., 1976. Stages in the Embryonic Development of the German Cockroach, *Blattella germanica* Linné (Blattaria, Blattellidae), vol. 44. Kontyû, Tokyo, pp. 1703–1714.

Tang, X., Engström, Y., 2019. Regulation of immune and tissue homeostasis by *Drosophila* POU factors. Insect Biochem. Mol. Biol. 109, 24–30.

Tidswell, O.R.A., Benton, M.A., Akam, M., 2021. The neuroblast timer gene *nubbin* exhibits functional redundancy with gap genes to regulate segment identity in *Tribolium*. Development 148, dev199719.

Tomoyasu, Y., Arakane, Y., Kramer, K.J., Denell, R.E., 2009. Repeated co-options of exoskeleton formation during wing-to-elytron evolution in beetles. Curr. Biol. 19, 2057–2065. https://doi.org/10.1016/j.cub.2009.11.014.

Truman, J.W., 2019. The evolution of insect metamorphosis. Curr. Biol. 29, 1252–1268.

Truman, J.W., Riddiford, L.M., 2019. The evolution of insect metamorphosis: a developmental and endocrine view. Philos. Trans. R. Soc. B Biol. Sci. 374, 20190070 https://doi.org/10.1098/rstb.2019.0070.

Truman, J.W., Riddiford, L.M., 1999. The origins of insect metamorphosis. Nature 401, 447–452. https://doi.org/10.1038/46737.

Turchyn, N., Chesebro, J., Hrycaj, S., Couso, J.P., Popadić, A., 2011. Evolution of nubbin function in hemimetabolous and holometabolous insect appendages. Dev. Biol. 357, 83–95.

Ventos-Alfonso, A., Ylla, G., Belles, X., 2019. Zelda and the maternal-to-zygotic transition in cockroaches. FEBS J 286, 3206–3221. https://doi.org/10.1111/febs.14856.

von Kalm, L., Crossgrove, K., Von Seggern, D., Guild, G.M., Beckendorf, S.K., 1994. The Broad-Complex directly controls a tissue-specific response to the steroid hormone ecdysone at the onset of *Drosophila* metamorphosis. EMBO J 13, 3505–3516.

Ylla, G., Piulachs, M.D., Belles, X., 2018. Comparative transcriptomics in two extreme neopterans reveals general trends in the evolution of modern insects. iScience 4, 164–179.

Zhou, B., Hiruma, K., Shinoda, T., Riddiford, L.M., 1998. Juvenile hormone prevents ecdysteroid-induced expression of broad complex RNAs in the epidermis of the tobacco hornworm, *Manduca sexta*. Dev. Biol. 203, 233–244.

Broad complex **and wing development in cockroaches**

Ana Fernandez-Nicolas, Alba Ventos-Alfonso, Orathai Kamsoi, Courtney Clark-Hachtel, Yoshinori Tomoyasu, Xavier Belles

SUPPLEMENTARY DATA

Table S1. Primers used for transcript measurements by qRT-PCR or to prepare riboprobe templates for *in situ* hybridization (ISH) in *Blattella germanica*.

Table S2. *In situ* hybridization protocol for *Blattella germanica* embryos.

Table S3. Primers used to prepare dsRNAs for RNAi in *Blattella germanica*.

Table S4. Summary of the different series of experiments carried out to study the phenotypic effects of the maternal RNAi of *Broad complex* (*Br-C*) in *Blattella germanica*.

Table S5. Summary of the experiments carried out to study the effects of nymphal RNAi combining the depletion of *Sex combs reduced* (*Scr*) and *Broad complex* (*Br-C*), and that of *nubbin* (*nub*), in *Blattella germanica*.

Fig. S1. Reads-based expression of wing-related genes obtained from the libraries of different embryo stages of *Blattella germanica* reported by Ylla et al. (2018).

Fig. S2. Expression profiles of *Br-C* and wing-related genes in the context of embryo development in *Blattella germanica*.

Fig. S3. Localization of *Br-C* transcripts by in situ hybridization (ISH) in embryos of *Blattella germanica*.

Fig. S4. Phenotypic effects of maternal RNAi of *Broad complex* (*Br-C*) in embryos of *Blattella germanica, as observed* 18 days after the formation of the ootheca, just before hatching under normal conditions.

Fig. S5. Phenotypic effects of maternal RNAi of *Broad complex* (*Br-C*) in embryos of *Blattella germanica*, as observed 60 h after the formation of the ootheca, that is at 15% total development, when the germ band is being formed.

Table S1. Primers used for transcript measurements by qRT-PCR or to prepare riboprobe templates for *in situ* hybridization (ISH) in *Blattella germanica*. In the primers sequence, "F" means forward, and "R" reverse.

Gene name	Reference sequence	Purpose	Primers sequence
actin 5c	AJ862721	qRT-PCR	F: 5'-AGCTTCCTGATGGTCAGGTGA-3' R: 5'-ACCATGTACCCTGGAATTGCCGACA-3'
apterous-a (*ap-a)*	LT216431.1	qRT-PCR	F: 5'-CGGACTACCTGGATGTTCCG R: 5'-TGGTTGATGGCGAAGTACGA
Broad Complex (BR-C) (core)	FN651774	qRT-PCR	F: 5'-CGGGTCGAAGGGAAAGACA-3' R: 5'-CTTGGCGCCGAATGCTGCGAT-3'
BR-C Z1	FN651774.1	qRT-PCR	F: 5'-CTTCAAGGGAGTACGGATGG-3' R: 5'-GGCGACGTAACCTCTGTAGC-3'
BR-C Z2	FN651775.1	qRT-PCR	F: 5'-CTTACCGGGAGTACGGATGG-3' R: 5'-ATGCTTGTCTGCAACGTGTC-3'
BR-C Z3	FN651776.1	qRT-PCR	F: 5'-CTTCAAGGGAGTACGGATGG-3' R: 5'-TGGAGGAGGGATGCGATAAT-3'
BR-C Z4	FN651777.1	qRT-PCR	F: 5'-CTTCAAGGGAGTACGGATGG-3' R: 5'-GAGAGGTAACTCGCCACTCG-3'
BR-C Z5	FN651778.1	qRT-PCR	F: 5'-CTTCAAGGGAGTACGGATGG-3' R: 5'-GCAGTAAGGAGGTCCACTGC-3'
BR-C Z6	FN651779.1	qRT-PCR	F: 5'-CTTCAAGGGAGTACGGATGG-3' R: 5'-CGCAGCTCATTTTGGATTTT-3'
Broad Complex (BR-C)	FN651774	ISH, riboprobe	F: 5'- GAGCGGTTTAACGCAACAAG-3' R: 5'- TGAAGACCCTGACCACCAAT-3'
Distal-less (Dll)	PYGN01000916.1	ISH, riboprobe	F: 5'- ATCAAGATTCGACGGCATCC-3' R: 5'- CCAAGAATACTGGGGCATGT-3'
nubbin (*nub*)	LT216433.1	qRT-PCR	F: 5'-CGTCACCAGAAGAAACAACAGA R: 5'-CGAGATTGTGGTCTGTGAGAAA
scalloped (*sd*)	HF969263.1	qRT-PCR	F: 5´-GCCCACAGAGTGCTTTCTTC-3´ R: 5´-CCCCTGCCTCATCTTGAATA-3´
Sex combs reduced (*Scr*)	LT216430.1	qRT-PCR	F: 5'-TGGATGAAGAGGGTGCATCT R: 5'-CTCAATCCTCCGTCTTCTGG
Ultrabithorax (Ubx)	LT216435.1	qRT-PCR	F: 5'-AAGAGGTCGCCAGACGTACA-3' R: 5'-TTGGAACCAAATTTTGATCTGTC-3'
vestigial (vg)	LN901335	qRT-PCR	F: 5'-AACTGTGTGGTGTTCACTCACT-3' R: 5'-AAGGAGGGAAGTTGCGAGC-3'
vestigial (vg)	LN901335	ISH, riboprobe	F: 5'-AACTGTGTGGTGTTCACTCACT R: 5'-AAGGAGGGAAGTTGCGAGC
wingless (*wg*)	HE965017.1	qRT-PCR	F: 5'- CTTGCAGGTGAAGACATGC R: 5'- TCGAAGCGGTCTTTGAGGTT

Table S2. *In situ* hybridization protocol for *Blattella germanica* embryos

Ana Fernandez-Nicolas & Courtney Clark-Hachtel, updated 21-12-2021. Tomoyasu lab, Miami University, Oxford, OH 45056, USA.

Embryo Fixation and Dissection:

1. _____ Remove oothecae from mother and place in PBT (PBS + 0.1% TritonX) in a 1.5 mL tube.
2. _____ Boil in PBT for 10 min.
3. _____ Transfer to ice immediately.
4. _____ Transfer all oothecae to 8% FA/PBT at room temperature (RT) and open each one.

   Fixative:
   - 1 mL 10x PBS
   - 8 mL 10% FA
   - 100 µL 10% Triton X
   - 1 mL 0.5 M EGTA
5. _____ When all are opened, transfer dish to ice.
6. _____ Dissect oothecae one by one in RT 8% FA/PBT.
7. _____ Once dissected, place embryos in cold fixative until all have been dissected.
8. _____ Transfer embryos to a glass vial.
9. _____ Replace cold fixative with RT 8% FA/PBT.
10. _____ Fix for 1hr at RT on a rotator.
11. _____ Remove fixative and replace with 100% MeOH, Shake for 30 sec.
12. _____ Remove MeOH and replace with 100% MeOH. Leave on rotator for 5 min.
13. _____ Remove and replace MeOH one more time before storing in -20°C.

------The following steps should be performed in an RNase-free environment------

Rehydration and Acetone treatment:

(All following steps should be performed with agitation unless otherwise specified)

1. _____ Transfer desired number of embryos to a 1.5mL tube.
2. _____, _____ Wash embryos with 100% ethanol for 2x5 min at RT.
3. _____ Incubate with xylene:ethanol (1:1 v/v) for 60 min at RT (Nagaso et al., 2001).
4. _____, _____ Wash embryos with 100% ethanol for 2x5 min at RT.
5. Gradual rehydration with:

   _____ 80% methanol/PTw 5 min at RT.

   PTw:
   - 500 µL 10% Tween 20
   - 50 mL PBS

   _____ 50% methanol/PTw 5 min at RT.

   _____ 25% methanol/PTw 5 min at RT.
6. _____ Treat with acetone (80%) 10 min at -20ºC.
7. _____, _____ Wash in PTw 2x5 min each.
8. _____ Post fix in 8% FA/PBS (no EGTA) for 20 min at RT.

   Fixative:
   - 4 mL 10% FA
   - 500 µL 10x PBS
   - 500 µL RNase free H2O

Prehybridization and Hybridization:
(All following steps should be performed with agitation unless otherwise specified)

1. _____, _____, _____ Wash in PTw 3x5 min at RT.
2. _____ Wash in PTw:Hybridization Buffer (Hyb) (1:1) 5 min at RT.
3. _____ Wash in Hyb for 5 min at RT.
4. _____ Replace Hyb. Prehyb embryos for 3 hours (55ºC).
5. _____ Boil 1.5 µl* of probe in 1 mL of Hyb Buffer for 5 min at 100ºC on the heat block.
   *Probe ratio can be changed. A ratio of 1:100 is commonly used for *Tribolium castaneum* (Shippy et al., 2009; Tomoyasu et al., 2009). When developing this protocol for *B. germanica*, we started from 0.5:1000 and adjusted from there based on staining and development time.
6. _____ Incubate on ice for 2 min.
7. _____ Incubate tissue o/n (55 ºC) in hyb/probe solution (at least 14 h).

------The following steps do not need to be in an RNase free environment------

Washing and Antibody Staining:
(All following steps should be performed with agitation unless otherwise specified)

1. _____ Wash in wash buffer I for 3 h at 55°C.
2. _____ Wash in wash buffer II for 3 h at 55°C.
3. _____ Wash in wash buffer III for 30 min at 55°C.
4. _____ Wash in wash buffer IV for 30 min at 55°C.
5. _____, _____ Wash in wash buffer V two times for 40 min each at 55°C.
6. _____, _____, _____ Wash in MA buffer + 0.1% Tween20 (MAw) at RT 3x5 min.
   MAw:
   - 0.5 mL 10% Tween in 50 mL MA buffer
7. _____ Incubate in blocking buffer for at least 1 h at RT.
   Blocking Buffer:
   - 500 µl NGS, 200 µl 10% Tween 20 in 10 mL of 5% Blocking reagent (Roche Applied Science 11096176001)
8. _____ Incubate with anti-DIG (1:2000 in blocking buffer) at 4°C overnight.

Color Development:

(BM purple)

1. _____, _____, _____, _____ Wash 4x10 min in MAw at RT on a rotator.
2. _____ Transfer embryos to glass viewing dish.
3. _____, _____ Wash 2x5 min in AP reaction buffer.
4. _____ Incubate in BM purple solution (Roche Applied Science 11442074001) for 30 min to overnight.
5. _____, _____, _____ Wash in PBT several times.
6. _____ Place tissues in 80% glycerol/PBS.

(Fast Red)

1. _____, _____, _____, _____ Wash 4x10 min in MAw @RT.
2. _____ Transfer embryos to glass viewing dish.
3. _____, _____, _____ Wash 3x5 min in 0.1M Tris-HCl pH8.0-8.2 + 0.1% Tween 20.
   - 1 mL of1 M Tris-HCl, 100 µl of 10% Tween 20 in 10 mL ddH20
4. _____ Dissolve Fast Red tablet (Sigma F4648) in 0.1M Tris-HCl pH8.0-8.2 + 0.1% Tween.
5. _____ Spin down the Fast Red solution.
6. _____ Stain embryos in Fast Red solution for up to 48h.
7. _____, _____, _____ Wash in PBT several times.
8. _____ Place embryos in 80% glycerol/PBS.

Reagents:

Hybridization Buffer:

50% formamide	100% solution	25 mL
5X SSC (pH 6.0)	20X SSC	12.5 mL
100 µg/µL Heparin	100 mg/mL	50 µL
0.1% Tween 20	10% stock	500 µL
100 µg/mL yeast RNA	10 mg/mL	500 µL
0.1% CHAPS	10% stock	500 µL
1X Denhart's	50X stock	1 mL
	Add RNAse free water to	50 mL

Wash Buffer

Wash Buffer I

50% formamide	100% solution	25 mL
5X SSC (pH 6.0)	20X SSC	12.5 mL
0.1% Tween 20	10% stock	500 µL
	Add water to	50 mL

Wash Buffer II

50% formamide	100% solution	25 mL
2X SSC (pH 6.0)	20X SSC	5 mL
0.1% Tween 20	10% stock	500 µL
	Add water to	50 mL

Wash Buffer III

25% formamide	100% solution	12.5 mL
2X SSC (pH 6.0)	20X SSC	5 mL
0.1% Tween 20	10% stock	500 µL
	Add water to	50 mL

Wash Buffer IV

2X SSC (pH 6.0)	20X SSC	5 mL
0.1% Tween 20	10% stock	500 µL
	Add water to	50 mL

Wash Buffer V

0.2X SSC (pH 6.0)	20X SSC	500 µL
0.1% Tween 20	10% stock	500 µL
	Add water to	50 mL

Maleic Acid Buffer (MA)

Maleic acid	11.61 g
NaCl	8.77 g/L

(adjust pH to 7.5 with 10 N NaOH)

AP Reaction Buffer (Make fresh before use)

100 mM Tris HCl pH 9.5	1 M stock	1 mL
100 mM NaCl	5 M stock	200 µL
50 mM MgCl2	1 M stock	500 µL
0.1% Tween 20	10% stock	100 µL
	Add water to	10 mL

References

Nagaso, H., Murata, T., Day, N., and Yokoyama, K.K. 2001. Simultaneous detection of RNA and protein by in situ hybridization and immunological staining. *J. Histochem. Cytochem.* 49: 1177–1182.

Shippy, T.D., Coleman, C.M., Tomoyasu, Y., and Brown, S.J. 2009. Concurrent in situ hybridization and antibody staining in red flour beetle (*Tribolium*) embryos. *Cold Spring Harb. Protoc.* 4:.

Tomoyasu, Y., Arakane, Y., Kramer, K.J., and Denell, R.E. 2009. Repeated co-options of exoskeleton formation during wing-to-elytron evolution in beetles. *Curr. Biol.* 19: 2057–2065.

Table S3. Primers used to prepare dsRNAs for RNAi in *Blattella germanica*. In the primers, sequence “F” means forward, and “R” reverse.

Gene name	Reference sequence	Primers sequence	Length (nt)
Autographa californica nucleopoydrovirus	K01149	F: 5’-ATCCTTTCCTGGGACCCGGCA-3’ R: 5’-ATGAAGGCTCGACGATCCTA-3’	306
Broad Complex (*BR-C*) (core)	FN651774	F: 5’-CATCAGAACAATCGCAGCATTC-3’ R: 5’-GAGAGTGACGATTGTTGATGG-3’	386
nubbin (*nub*)	LT216433.1	F: 5’-ACGAATCTTGGAACCGTCAC-3’ R: 5’-TGCAATTTCTTCCGATGTTG -3’	406
Sex combs reduced (*Scr)*	LT216430.1	F: 5’-CTCAGCAAGTCCCTGGTCAT-3’ R: 5’-AATCGGGGGACTACTCCTTG-3’	386

Table S4. Summary of the different series of experiments carried out to study the phenotypic effects of the maternal RNAi of *Broad complex* (*Br-C*) in *Blattella germanica*. The embryos were examined 18 days after the formation of the ootheca, just before hatching under normal conditions. The phenotypes 1-4 are described in Fig. S1.

dsRNA	Series	Oothecae studied	Embryos examined	Phenotype 1	Phenotype 2	Phenotype 3	Phenotype 4
dsBrC	1	6	128	31 (24.2%)	0	10 (7.8%)	87 (68.0%)
dsMock	1	6	200	0	0	0	200 (100%)
dsBrC	2	6	204	50 (24.5%)	15 (7.4%)	0	139 (68.1%)
dsMock	2	6	206	0	0	0	206 (100%)
dsBrC	3	8	277	128 (46.2%)	4 (1.4%)	1 (0.4%)	144 (52.0%)
dsMock	3	5	190	0	0	0	190 (100%)
dsBrC	4	6	213	118 (55.4%)	0	0	95 (44.6%)
dsMock	4	5	190	0	0	0	190 (100%)
dsBrC	5	6	206	55 (26.7%)	5 (2.4%)	6 (2.9%)	140 (68.0%)
dsMock	5	6	198	0	0	0	198 (100%)
dsBrC	**1-5**	**32**	**1028**	**382 (37.2%)**	**24 (2.3%)**	**17 (1.7%)**	**605 (58.8%)**
dsMock	**1-5**	**28**	**984**	**0**	**0**	**0**	**984 (100%)**

Table S5. Summary of the experiments carried out to study the effects of nymphal RNAi combining the depletion of *Sex combs reduced* (*Scr*) and *Broad complex* (*Br-C*), and that of *nubbin* (*nub*), in *Blattella germanica*. The dsRNAs (gene specific or control: dsMock) weres injected into the abdomen of nymphs. Three successive treatments were made, in the fourth, five and sixth nymphal instar, freshly emerged in all cases. The phenotypes were observed after the imaginal molt and are depicted in Fig. 4 (*Scr* and *Br-C*), and Fig. 5 (*nub*).

Treatment	n	Main phenotypical trait
RNAi experiments *Scr* and *Br-C*		
3 µg dsScR + 3 µg dsMock	28	Pronotum showing conspicuous latero-posterior expansions of the pronotal edge .
3 µg dsScR + 3 µg dsBrC	34	Pronotum showing conspicuous latero-posterior expansions, but less pronounced than those obtained by depleting only Scr
3 µg dsBrC + 3 µg dsMock	24	Pronotum normal, with rounded sides, not latero-posteriorly expanded.
6 µg dsMock	19	Pronotum normal, with rounded sides, not latero-posteriorly expanded.
RNAi experiments *nub*		
3 µg dsnub	23	Wings (tegmina and membranous) smaller than controls
3 µg dsMock	16	Wings normal

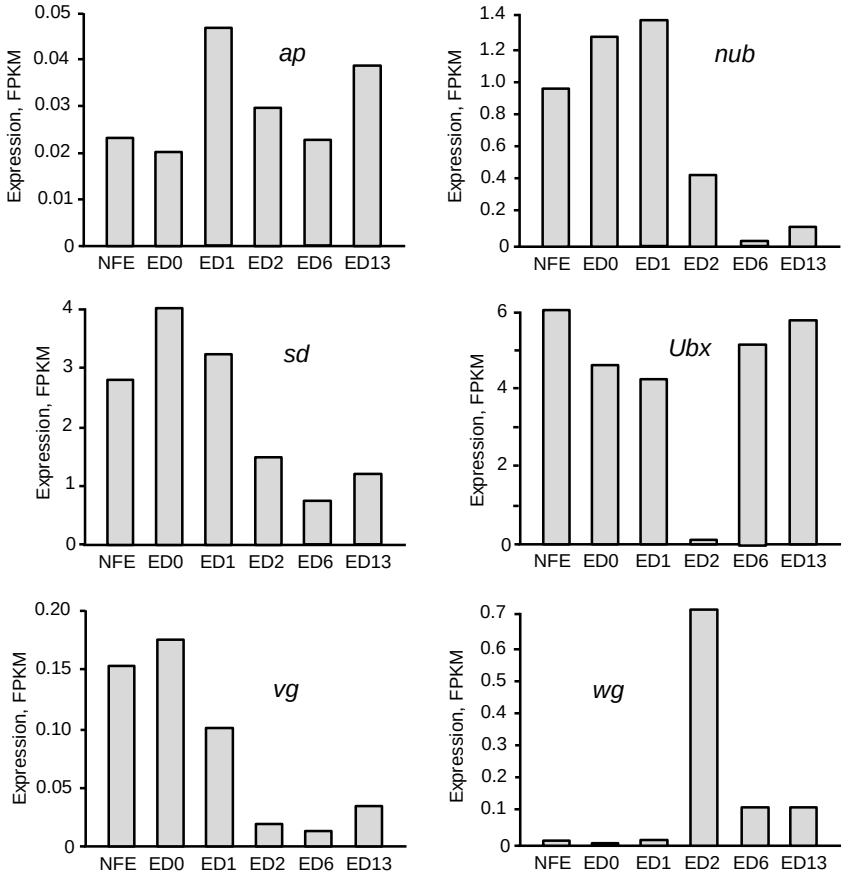

Fig. S1. Reads-based expression of wing-related genes obtained from the libraries of different embryo stages of *Blattella germanica* reported by Ylla et al. (2018). The expression is indicated as Fragments Per Kilobase Million (FPKM)

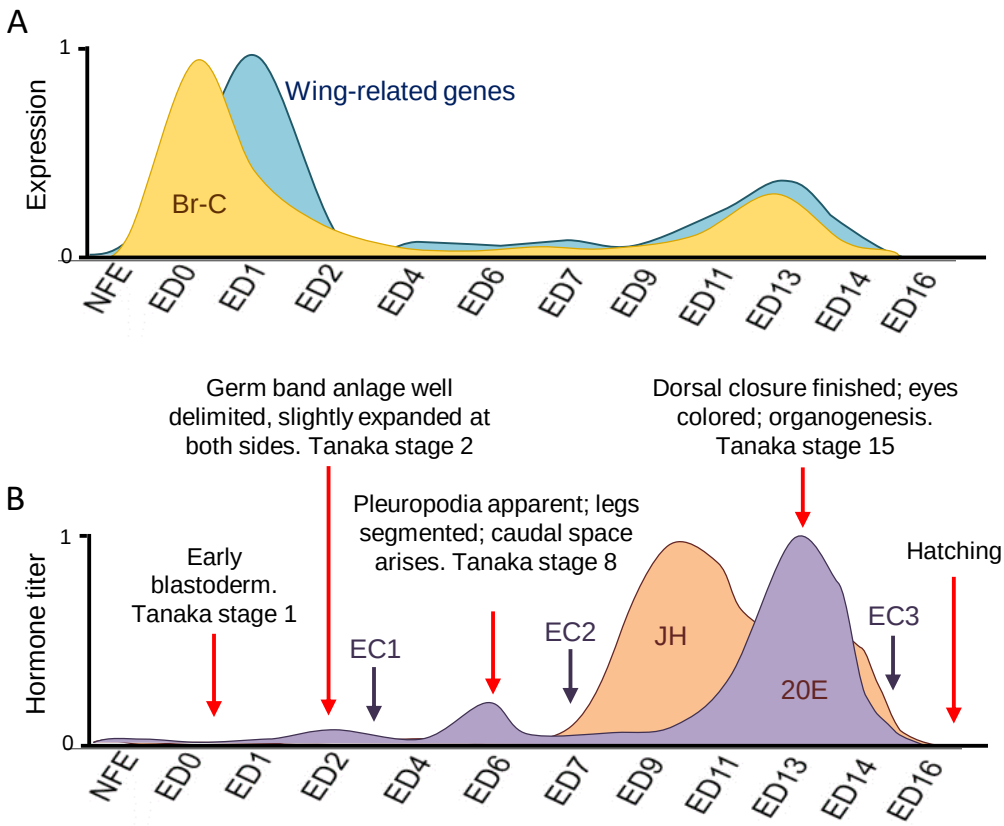

Fig. S2. Expression profiles of *Br-C* and wing-related genes in the context of embryo development in *Blattella germanica*. A. Scheme of the expression profiles of *Br-C* and the studied wing-related genes throughout embryogenesis, from "Non fertilized eggs" (NFE) and embryo day 0 (ED0), to ED16. B. Circulating levels of juvenile hormone (JH, data from Maestro et al. (2010) and ecdysteroids (20E, data from Maestro et al, 2005) throughout embryogenesis. The main developmental events are also indicated, using the stages defined by Tanaka (1976). EC indicates the deposition of the three successive embryonic cuticles. The levels of expression and of hormones are shown in relative values, referring to the value 1 the maximum levels in all profiles.

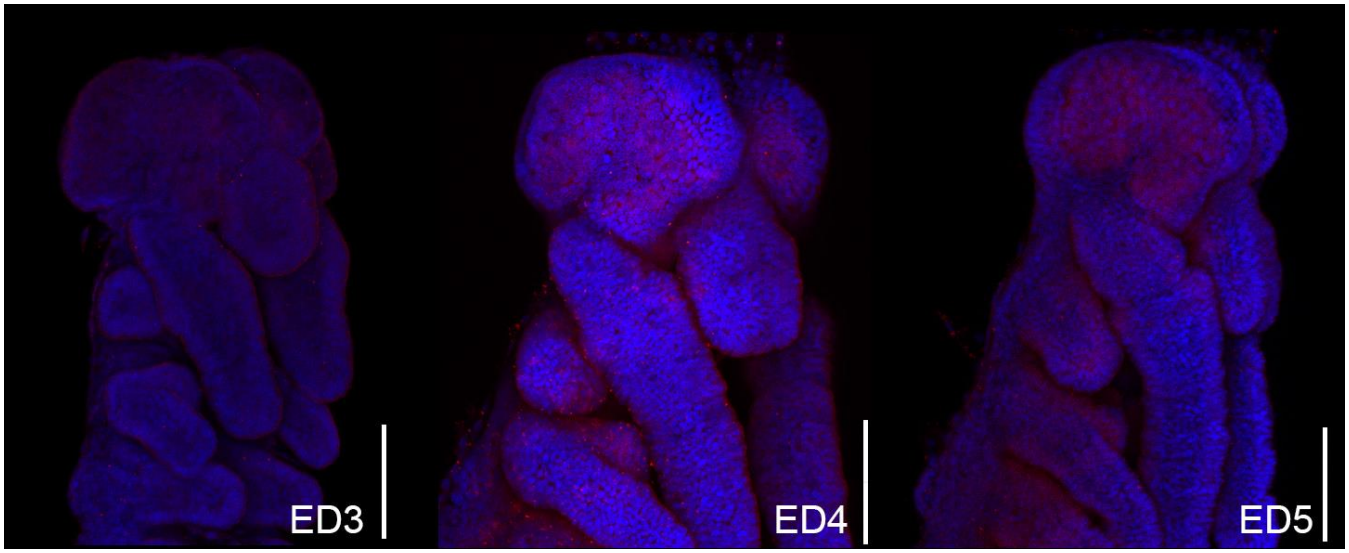

Fig. S3. Localization of *Br-C* transcripts by in situ hybridization (ISH) in the cephalic region of *Blattella germanica* embryos. ISH was carried out on 3-, 4- and 5-day-old embryos (ED3, ED4 and ED5). Blue: DAPI staining; red: ISH labeling. The *Br-C* riboprobe was designed within the core region, thus it reveals all *Br-C* isoforms. Scale: 100 µm.

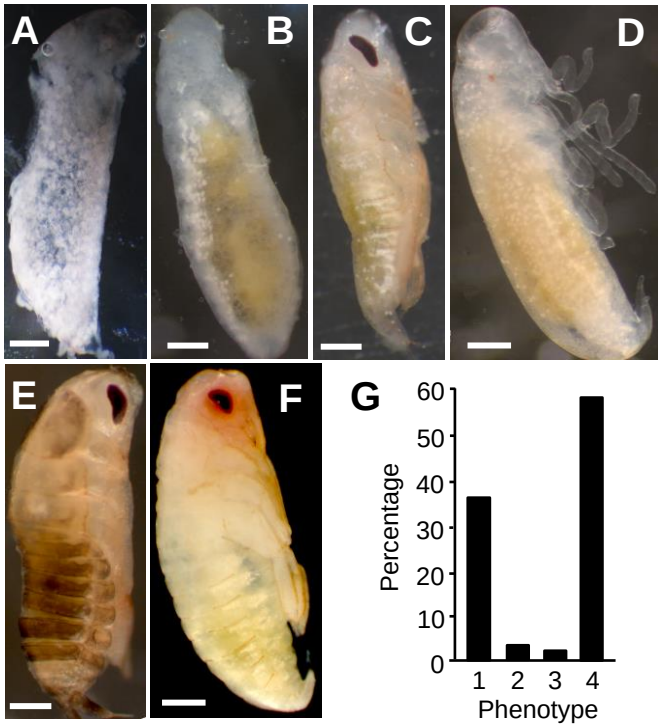

Fig. S4. Phenotypic effects of maternal RNAi of *Broad complex* (*Br-C*) in embryos of *Blattella germanica, as observed* 18 days after the formation of the ootheca, just before hatching under normal conditions. We studied 32 oothecae produced by dsBrC-treated females and 28 oothecae from control (dsMock-treated) females. From the 32 *Br-C* depleted oothecae, we studied 1028 embryos, which showed a diversity of phenotypes and a certain variability between series of experiments (see Table S4). A total of 382 embryos (37.2%) did not show an identifiable germ-band anlage, thus we infer that they had interrupted development between stages 1 and 2 (phenotype 1, panel A). A total of 24 embryos (2,3%) were segmented and had appendages, showing interrupted development between Tanaka stages 10 and 15, including diverse malformations, such as short appendages, reduced abdomen or imperfect eyes (phenotype 2, panels B, C, D). A total of 17 embryos (1.7%) were apparently well formed nymphs, but featured an intensely sclerotized cuticle (phenotype 3, Panel E). Finally, 605 embryos (58.8%) were apparently well formed nymphs (phenotype 4, Panel F). The observed percentage of each phenotype is summarized in panel G. Scale bars: 300 µm.

To examine the embryos, the oothecae were opened after 5 min in a water bath at 95ºC and the embryos were dechorionated and individualized. Then, they were fixed in 4% paraformaldehyde for 2 h, washed with 0.2% PBT, and examined and photographed in a Stereomicroscope DiscoveryV8 (Carl Zeiss MicroImaging).

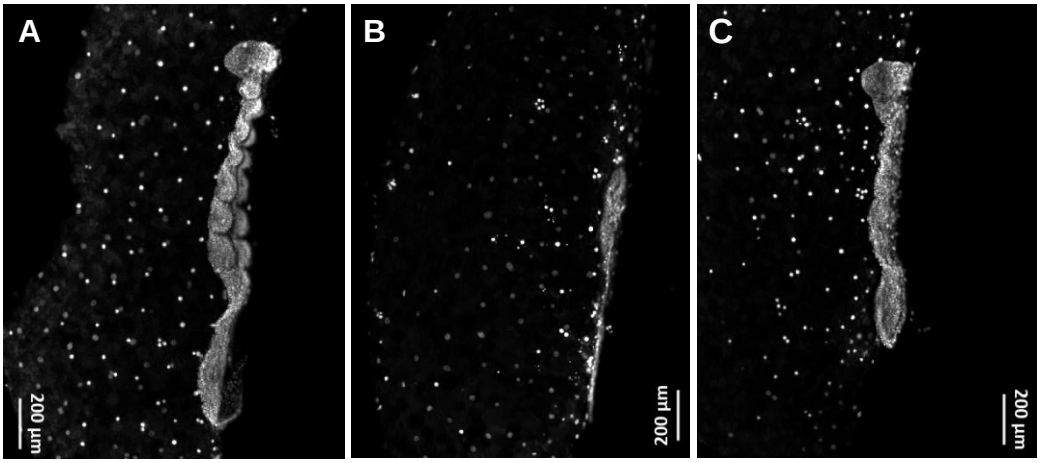

Fig. S5. Phenotypic effects of maternal RNAi of *Broad complex* (*Br-C*) in embryos of *Blattella germanica*, as observed 60 h after the formation of the ootheca (AOF), that is at 15% total development, when the germ band is being formed. A total of six othecae from females treated with dsMock were dissected, and 148 embryos from these oothecae were examined. All them had formed the germ band, showing the cephalic and thoracic segments clearly segmented, and the abdominal region still amorphous (Panel A), as normal at this stage. In parallel, we obtained six othecae from females treated with dsBrC, from which we dissected 152 embryos 60 h AOF. From these, 89 embryos (58.6%) had formed a normal germ band, with the cephalic and thoracic segments clearly segmented, like in controls, whereas 63 embryos (41.4%) had formed a defective germ band, very thin and practically amorphous (Panel B) or something thicker, with the cephalic and thoracic segmentation absent or very little marked (Panel C). DAPI staining was used in all cases. Scale bars: 200 µm.

To examine the embryos microscopically, the oothecae were opened after 5 min in a water bath at 95ºC and the embryos were dechorionated and individualized. Then, they were fixed in 4% paraformaldehyde, permeabilized in PBS-0.2% tween (PBT) and incubated for 10 min in 1 µg/ml DAPI in PBT. They were then mounted in Mowiol (Calbiochem, Madison, WI, USA) and examined and photographed using epifluorescence with an AxioImager Z1 microscope (ApoTome System, Zeiss).